Chemically functionalized magnetic exchange interactions of hybrid organic-ferromagnetic metal interfaces

Rico Friedrich, Vasile Caciuc, Nikolai S. Kiselev, Nicolae Atodiresei, and Stefan Blügel

Chemically functionalized magnetic exchange interactions

of hybrid organic – ferromagnetic metal interfaces

Rico Friedrich,[1, *] Vasile Caciuc,[1] Nikolay S. Kiselev,[1] Nicolae Atodiresei,[1, †] and Stefan Blügel[1]

[1] *Peter Grünberg Institut (PGI-1) and Institute for Advanced Simulation (IAS-1),*

Forschungszentrum Jülich and JARA, D-52425 Jülich, Germany

Abstract

We theoretically explore through systematic multiscale *ab initio* and Monte Carlo calculations how the surface magnetism of a ferromagnetic surface can be fine-tuned by nonmagnetic organic molecules containing a single π-bond. We demonstrate that a magnetic hardening or softening can be induced depending on the electronegativity of the heteroatom or when the π-bond "bridges" the magnetic surface atoms. Finally, the Monte Carlo simulations revealed taylored macroscopic hysteresis loops corresponding to soft and hard molecule-surface magnets.

I. INTRODUCTION

Organic and molecular spintronics aim at integrating the spin degree of freedom in electronic devices by making use of the spin-dependent properties of magnetic hybrid organic-metal interfaces[1–4]. The feasibility of these fields was demonstrated by the preparation of an exciting device, an organic-based spin-valve[5], where an organic layer was placed between two ferromagnetic contacts so that a giant magnetoresistance (MR) signal could be measured at low temperature[6]. Very recently, organic spin-valve devices with a large interfacial MR response even at room temperature[7] or an improved air-stability[8] have also been designed. Furthermore, single molecule magnets have been employed to design supramolecular spin-valve devices[9] or have been integrated in a three-terminal device to access the nuclear spin state of a Tb atom[10].

A major challenge in organic and molecular spintronics is to provide a clear physical picture of the basic mechanisms that govern the spin injection into the organic layer and the subsequent spin transport process[11,12]. In this respect, a key feature of such organic spintronic systems is the presence of a hybrid molecule-metal interface formed upon molecular adsorption that crucially controls their properties[13–16]. For instance, for π-conjugated organic molecules on magnetic surfaces the spin polarization at the molecular site can even be inverted with respect to the polarization of the substrate[15–17] and this effect can be tailored by a chemical functionalization process[18].

It is important to note that so far most experimental and theoretical studies have been focused on the transport properties of hybrid molecule-surface systems while much less explored is how the molecule-surface interactions alter the magnetic properties of the underlying substrate. In this respect, in a recent theoretical study it was clearly demonstrated that the adsorption of a non-magnetic organic molecule such as paracyclophane on a magnetic surface can locally strengthen the magnetic exchange interaction between the surface atoms directly interacting with the π-conjugated molecule[19]. This possibility to locally induce an increase (magnetic *hardening* effect) or decrease (magnetic *softening* effect) of the magnetic exchange coupling J opens a new and exciting path to engineer the surface magnetic properties via molecular adsorption[20]. Interestingly, direct consequences of the increased surface exchange coupling constants are an increased Curie temperature[19] and an opening of the magnetic hysteresis loop, i.e. an enhanced coercive field, of organic material-magnetic

2

39 surface systems with respect to the clean substrate one[20–23].

40   The next necessary step to bring these molecule-induced magnetic effects towards po-
41 tential technological applications is to provide a practical recipe how to tune the molecule-
42 surface interaction to obtain hybrid molecular-based systems with a specific magnetic behav-
43 ior. Therefore, in this first-principles study we focused on the engineering of the magnetic
44 properties of molecule-surface systems by systematically investigating the role played by
45 heteroatoms within π-bonded organic molecules on the change of the surface magnetic ex-
46 change coupling constants J. In particular, we have chosen to investigate a set of chemically
47 functionalized non-magnetic π-bonded molecules on 1 ML Fe on a W(110) substrate since
48 this is a commonly selected prototype system of a thin ferromagnetic film with an in-plane
49 magnetization[24]. Note also that for this surface the magnetic hardening of the Fe intra-layer
50 J due to the adsorption of organic molecules has been already demonstrated[19].

51   To unveil a clear recipe how to (i) induce a magnetic hardening and/or softening effect
52 and (ii) tune their magnitude in a magnetic surface or thin film due to its interaction
53 with non-magnetic π-conjugated molecules, we analyzed in detail how the surface magnetic
54 properties are locally modified in the presence of the simplest π-bonded molecular systems
55 possible. In practice this means that one starts with a molecule that has only one bonding
56 π molecular orbital (MO), i.e., ethene (C_2H_4). The advantage of this starting point is that
57 in a simple fashion hetero analogues can be derived by just exchanging one carbon atom
58 by a specific hetero element as B, N or O [see Fig. 1(a)]. The basic aim of this chemical
59 functionalization process is twofold: (i) to tailor the energetic position of the π MOs between
60 the different systems and thus to tune the strength of the molecule surface interaction[25]
61 and (ii) to use elements with a different chemical reactivity (electronegativity) to *locally*
62 modify the magnetic interactions between the surface Fe atoms via a specific heteroatom-Fe
63 hybridization.

64   Our *ab initio* results show that not only the strength of the magnetic hardening effect
65 can be tuned as a function of the chemical electronegativity of the heteroatom but also that
66 a magnetic softening effect can be achieved depending on (i) the nature of the heteroatom
67 or (ii) by a specific molecular adsorption geometry. Furthermore, we demonstrate by tak-
68 ing into account only the geometrical distortions on the magnetic surface induced by the
69 organic molecules that these do not account for the observed changes in J with respect to
70 its clean surface value. In particular, our theoretical study reveals that especially the *local*

3

71 hybridization between a specific heteroatom and the substrate are of crucial importance to 72 strengthen or weaken the magnetic coupling between the surface Fe atoms. Finally, based 73 on Monte Carlo simulations using a Heisenberg model with first principles parameters we 74 demonstrate that the considered set of functionalized π-conjugated molecules allows to tune 75 the coercive field over a large temperature range essentially via the modified J.

II.   COMPUTATIONAL DETAILS

77   Our spin-polarized electronic structure calculations were carried out within the framework 78 of the density functional theory[26,27] using the VASP program[28,29]. In addition, the projector 79 augmented-wave (PAW) method[30] was used with projectors as constructed for the exchange- 80 correlation functional of Perdew, Burke and Ernzerhof (PBE)[31].

81   Throughout all calculations the wave functions were expanded into plane waves with a 82 cutoff of 500 eV. All structures were relaxed until the forces excerted on the atoms were 83 smaller than 1 meV/Å. Concerning the Brillouin-zone integration, for the structural relax- 84 ations only the Γ-point was taken into account, whereas the calculation of the projected 85 density of states, the different antiferromagnetic configurations to obtain the exchange cou- 86 pling constants and the magnetic anisotropy were carried out with a k-point set of $4 \times 5 \times 1$. 87 In our *ab initio* calculations the unit cell consisted of one Fe layer and six W layers each 88 represented by a 3×4 in-plane unit cell containing 24 Fe or W atoms per layer. The vacuum 89 distance along the axis z perpendicular to the surface plane separating the supercells was 90 about 16 Å. The distance between molecules in the neighboring unit cells was at least about 91 10 Å. During the geometry optimization the upper three W layers, the Fe layer and the 92 molecular coordinates were allowed to relax.

III.   RESULTS AND DISCUSSION

94   To start with the first goal of the chemical functionalization process, in Fig. 1(b) the 95 calculated energy level spectra of the resulting set of π-conjugated molecules are presented. 96 As expected, the bonding π- as well as the antibonding π^*-states are lowered in energy when 97 going from methyleneborane (CH$_3$B) to formaldehyde (CH$_2$O) since the core potential of 98 elements with higher atomic number is more attractive which goes along with an increase in
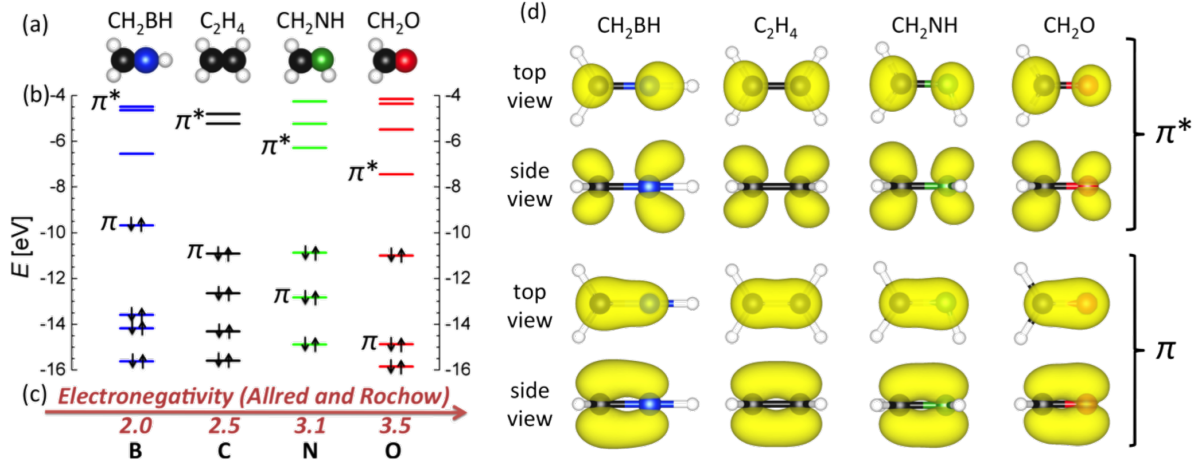
FIG. 1. (a) Chemical formula and atomic structure of methyleneborane (CH_3B), ethene (C_2H_4), methyleneimine (CH_3N) and formaldehyde (CH_2O). Color code: gray for hydrogen, black for carbon, blue for boron, green for nitrogen and red for oxygen. (b) Energy level diagram for the molecules in gas phase presented in (a). The bonding π-state as well as the antibonding π^*-state is labeled for each system. The occupation of the states is marked by arrows. Note that the highest occupied molecular orbital (HOMO) of each molecule has been aligned at its calculated ionization potential. (c) Electronegativity scale for the elements taking part in the formation of the π-bond. The values for the atomic electronegativities were taken from Ref.33. (d) The charge density plots show that the specific chemical reactivity of the heteroatom is directly reflected by the spatial extent of the bonding π- and antibonding π^*-states.

99 electronegativity [see Fig. 1(c)]. Hence using different hetero elements allows us to tune the
100 energetic position as well as the spatial extend of the bonding π- and antibonding π^*-states
101 [see Fig. 1(d)].

102   To identify the structural ground states of the different molecules adsorbed on 1 ML Fe
103 on W(110), six different adsorption sites have been considered by placing the π-bond of each
104 molecular system initially either on top of an atom or between two, three or four ferromag-
105 netic Fe atoms. The relaxed ground state geometries obtained for the different systems are
106 depicted in Fig. 2(a)-(d). Obviously for ethene, methyleneimine and formaldehyde adsorbed
107 on the Fe/W(110) surface [Fig. 2(b)-(d)] the π-bond is most favorably placed between three
108 iron atoms. These three iron atoms are also pulled closer together as a consequence of the
109 molecular adsorption (see Table III in appendix C for relaxed Fe-Fe distances.). However, in
110 case of methyleneborane the boron atom adsorbs into the hollow created by the three iron
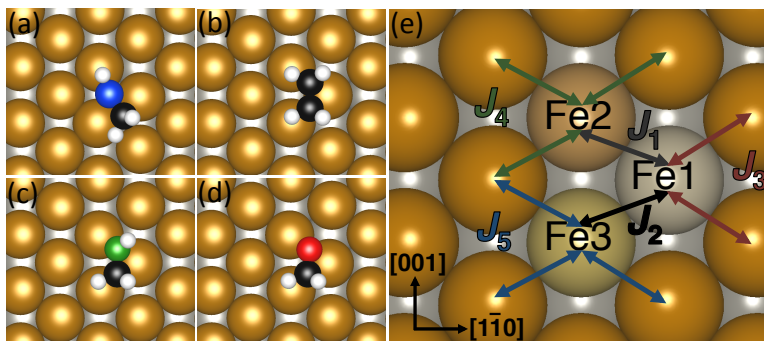
5

FIG. 2. Optimized ground state structures for (a) methyleneborane (CH$_3$B), (b) ethene (C$_2$H$_4$), (c) methyleneimine (CH$_3$N) and (d) formaldehyde (CH$_2$O) on 1 ML Fe/W(110). (e) Labeling of the three surface Fe atoms which are influenced by the adsorption of the molecules in their stable geometry. The different exchange coupling constants J are also indicated. Note that these images have been obtained with the VESTA program[34].

111 atoms under the molecule that consequently relax away from the boron atom.

112 The adsorption energies for the optimized structures are presented in Table I. Follow-
113 ing the discussion of the energetic position of the π MOs in the gas phase [see Fig. 1(b)],
114 methyleneborane interacts most strongly with the surface whereas the adsorption energies of
115 all other molecules are considerably smaller. Nevertheless, adsorption energies of more than
116 1 eV for such small molecular systems already point to chemisorption as bonding mechanism.

117 As regarding the aim to functionalize the C$_2$H$_4$ molecule to locally modify the surface
118 magnetic properties, all considered molecules have a pronounced influence on the magnetic
119 moments of the surface Fe atoms. More precisely, in all cases only the three surface Fe
120 atoms close to the organic molecules labeled as Fe1, Fe2 and Fe3 are affected as illus-
121 trated in Fig. 2(e). In Table I the magnetic moments of these Fe atoms below the π-bonded
122 molecules are listed. The general trend is that the calculated magnetic moments are smaller
123 than the value of 2.5 μ_B for clean Fe/W(110). This reduction is due to the hybridization

6

TABLE I. Adsorption energy E_{ads} for each system (given in eV), magnetic moments of the three Fe atoms in the vicinity of the π-bonded molecules (given in μ_{B}) and calculated exchange coupling constants J between the Fe atoms for the molecules on the surface and the clean Fe/W(110) surface geometries induced by the π-conjugated molecules (all in meV/μ_{B}^2). Note that the adsorption energy is defined as $E_{\mathrm{ads}} = -(E_{\mathrm{sys}} - (E_{\mathrm{surf}} + E_{\mathrm{molec}}))$, where E_{sys} is the total energy of the molecule-surface system, E_{surf} represents the total energy of the Fe/W(110) surface and E_{molec} corresponds to the total energy of the molecules in the gas phase.

molecule/surface		E_{ads}	magnetic moments			molecule/surface					induced geometry				
			Fe1	Fe2	Fe3	J_1	J_2	J_3	J_4	J_5	J_1	J_2	J_3	J_4	J_5
clean surface		-	2.5	2.5	2.5	5.9	5.9	5.9	5.9	5.9	5.9	5.9	5.9	5.9	5.9
methyleneborane	(CH$_3$B)	3.30	2.0	2.0	2.1	15.7	1.0	7.1	7.1	12.2	4.0	3.9	4.6	5.8	6.4
ethene	(C$_2$H$_4$)	1.19	2.2	2.1	2.1	15.4	15.4	5.9	8.6	8.6	8.3	8.3	2.2	5.5	5.5
methyleneimine	(CH$_3$N)	1.76	2.2	2.3	2.0	6.4	11.0	9.6	8.1	7.9	5.9	7.0	3.3	5.6	5.3
formaldehyde	(CH$_2$O)	1.48	2.3	2.5	2.0	3.9	11.9	8.8	8.0	8.4	6.8	6.0	2.9	6.3	5.1

between the Fe-d states mainly with the p_z-like atomic orbitals of carbon and heteroatoms, respectively. Remarkably, the magnetic moment of Fe2 that is close only to the molecular heteroatom increases towards the value of the clean surface when going from methyleneborane to formaldehyde suggesting a decrease of the heteroatom influence on the magnetic properties of the surface starting from B to O. This intriguing behavior can be assigned to an interplay between (i) a generally smaller heteroatom-Fe2 distance than the C-Fe ones (see Table III in appendix C) and (ii) a lowering of the energetic position of the p_z orbitals starting from B to O as depicted in Fig. 1(b) for the corresponding π MOs. A similar, albeit weaker trend is observed for the Fe1 atom while in the case of Fe3 close only to the carbon atom its magnetic moment remains almost the same for all molecules considered in our study. This observation already suggests a *local reactivity-dependent* impact of the heteroatom on the magnetic properties of the Fe surface.

A smaller value of the surface magnetic moments can also change the strength of the Fe-Fe magnetic interaction with respect to the clean surface case. In consequence, we now thoroughly investigate the impact of the heteroatom in organic molecules with a single π-bond onto the magnetic exchange coupling constants J between the Fe atoms of the

substitute. As in Ref.19, we describe the exchange coupling between the magnetic moments of the Fe atoms by an effective classical Heisenberg Hamiltonian $H = -\sum_{i>j} J_{ij} \, \mathbf{m}_i \, \mathbf{m}_j$ taking into account only nearest neighbors, where $\mathbf{m}_i$ and $\mathbf{m}_j$ stand for the magnetic moments at sites i and j, respectively. Using this Heisenberg Hamiltonian, for a set of antiferromagnetic configurations a linear system of equations is obtained to determine the different parameters J labeled in Fig. 2(e) (see appendix A for more details). The calculated exchange coupling constants for the molecule-Fe/W(110) systems are presented in Table I and are also visualized in Fig. 3(a). Note that the calculated clean surface coupling constant is 5.9 meV/μ_B^2 and is also included in Fig. 3 as a reference[35].
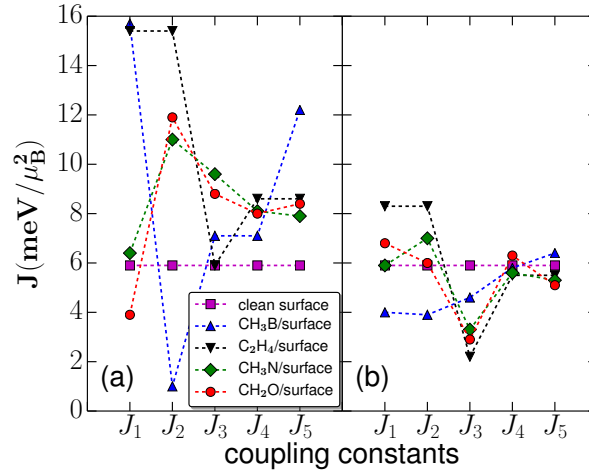

FIG. 3. Visualization of the calculated magnetic exchange coupling constants for (a) the molecules on the surface and for (b) the surface geometries induced by the respective molecules with the molecules removed. Remarkably, the coupling constants for the induced geometries in (b) do not reproduce the coupling constants of the hybrid systems in (a). This difference highlights the importance of the molecule-substrate hybridization for the calculated surface exchange coupling constants J.

In general, the calculated exchange coupling constants using the procedure outlined above are considerably enhanced as compared to the clean substrate value and this behavior is particularly pronounced for the ethene system with obtained values of $J_1 = J_2 = 15.4$ meV/μ_B^2. These Js are similar to the value of 15.65 meV/μ_B^2 evaluated for the paracyclophane molecule in Ref.19 that also does not contain heteroatoms. Besides this, the J_2 for methyleneimine and formaldehyde is also significantly enhanced to 11.0 meV/μ_B^2 and 11.9 meV/μ_B^2, respectively,

8

as compared to the clean surface value. On the other hand, J_1 systematically decreases when going from methyleneborane to formaldehyde (from 15.7 meV/μ_B^2 to 3.9 meV/μ_B^2). Interestingly, we note that this decrease of J_1 correlates to an increase of the heteroatom electronegativity. In particular, for formaldehyde containing the heteroatom (O) with the largest electronegativity the $J_1 = 3.9$ meV/μ_B^2 is *smaller* than the coupling constant of the clean surface revealing a magnetic softening of the Fe-Fe exchange coupling due to oxygen. Since the surface Fe1-Fe2 and Fe1-Fe3 magnetic interactions leading to the calculated Js are mediated by hetero and C atoms, respectively, (see Fig. 2 and the discussion below) this behavior fundamentally shows that it is indeed possible to locally tune the magnetic exchange coupling of a surface by decorating it with suitable adsorbates.

In contrast, the methyleneborane case is again qualitatively different. The J_1-coupling mediated by the B atom is slightly larger than that of ethene but the J_2 coupling which is mediated by both the B and C atoms [see Fig. 2(a)] is drastically decreased to only about 1 meV/μ_B^2. Therefore, from these results it can be deduced that if not only a single atom as O but a whole B–C bond mediates the magnetic interaction between two Fe atoms, the coupling can be significantly weakened. Besides this, the other coupling constants J_3 to J_5 are also slightly larger than the clean surface value for all the hybrid systems investigated in our study.

As regarding the mechanism of the magnetic hardening of the surface exchange coupling constants J due to molecular adsorption, the crucial role played by the hybridization between the out-of-plane Fe d-like atomic orbitals and the p_z ones of the molecular atoms was emphasized in Ref.19. In the following we will denote this contribution to the surface magnetic hardening as a molecule-surface hybridization effect.

Furthermore, we address the question which contribution to J results from the changes in the Fe-Fe interaction due to the surface distortions induced upon molecular adsorption, a contribution denoted as a geometrical effect. To investigate this issue, we have performed similar calculations of the exchange coupling constants for each relaxed Fe/W(110) surface by removing the molecules from our systems. We note that for these induced geometries the magnetic moments of the Fe atoms with distorted positions deviate only negligibly from the clean surface moment of 2.5 μ_B.

The calculated exchange coupling constants J are reported in Table I and their magnitude is depicted in Fig. 3(b). As a general feature, the exchange coupling constants J_1 and J_2 eval-

uated for the ethene-, methyleneimine- and the formaldehyde-induced surface geometries are typically larger than the corresponding clean surface value. Importantly, they do not reach the values obtained with molecules adsorbed on the surface. Besides this, J_3 is considerably smaller for all three systems while J_4 and J_5 are close to the clean surface value. Overall, this behavior can be correlated with the geometrical distortions on the surface induced by the molecules. More specifically, all three molecules distort the surface in such a fashion that Fe1 is pulled closer to Fe2 and Fe3 (see Table III in appendix C) thereby enhancing the Fe-Fe magnetic couplings J_1 and J_2. The resulting enhanced distance of Fe1 to the unperturbed surface neighbors (more than 2.8 Å see Fig. 2) leads then to the weakening of J_3. Furthermore, the distances of Fe2 and Fe3 to their unperturbed surface neighbors are practically unaffected and therefore the J_4 and J_5 exchange coupling constants are similar to their clean surface counterparts, as already mentioned. For the methyleneborane-induced geometry the situation is different. In this case the J_1 and J_2 are decreased, whereas J_3 to J_5 are quite close to the clean surface value. This is due to the fact that the B atom in Fig. 2(a) pushes Fe1, Fe2 and Fe3 apart, which leads to a weakening of their magnetic coupling. But on the other hand Fe3 is also pushed towards its clean surface neighbors which leads to a slight enhancement of J_5.
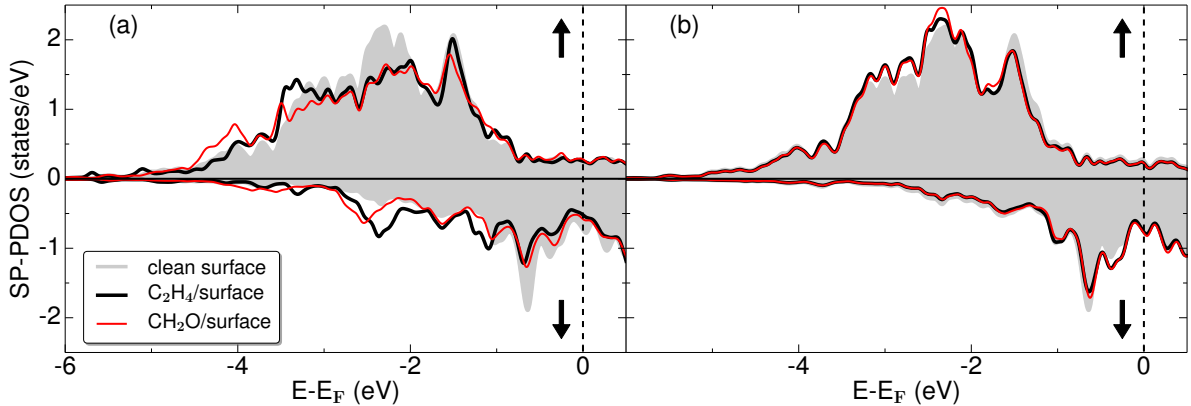

FIG. 4.   Spin-polarized projected density of states (SP-PDOS) obtained for the d-states of Fe1 in the case of (a) molecule/surface and (b) molecular-induced surface geometries. For the sake of clarity only the results for the C_2H_4 and CH_2O systems are shown. Note that the differences between the SP-PDOS in (a) and (b) are responsible for the large differences in J evaluated for the corresponding systems as shown in Table I.

As depicted in Fig. 4, this difference between the full molecule-surface and surface-

distorted only systems is also qualitatively illustrated by the analysis of the spin-polarized projected density of states (SP-PDOS) evaluated for the d-states of the surface Fe1 atom. Conclusively, as compared to the d SP-PDOS of a clean surface atom, in the case of molecule-surface systems [see Fig. 4(a)] the d-states of Fe1 are significantly hybridized mainly with the p_z-like orbitals of molecular atoms while these d-states look almost similar to the clean surface one for the corresponding molecular-induced surface geometries [see Fig. 4(b)]. However, it is very important to emphasize that these small differences in the d SP-PDOS between the molecular-induced surface systems are still responsible for the significant differences between their calculated exchange coupling constants J and that of the clean surface as depicted in Table I.

Another important magnetic property is the magnetic anisotropy of the molecule-metal hybrid systems under consideration, i.e., we address here the question in which extent the adsorption of the molecules can change the magnetization direction at the Fe surface (a question that also determines the stability against the switching of the magnetization). In consequence, we calculated the magnetocrystalline anisotropy energies[32] (MAEs) as total energy differences with magnetization directions along the three high symmetry directions, the in-plane directions [1$\bar{1}$0], [001] and the out-of-plane direction [110] for all molecules on the Fe/W(110) surface by taking into account the spin-orbit coupling. The obtained results are presented in Table II. We note that our MAE evaluated for the clean surface (2.7 meV) is very close to the one obtained by the linearized augmented plane wave method (2.8 meV)[24]. In all cases the easy axis of the system is the in-plane [1$\bar{1}$0] direction (long axis of a c(2×2) surface unit cell), which is the same as for the clean surface. However, importantly, our *ab initio* calculations suggest that the hard axis is changed upon molecular adsorption in the case of the methyleneborane and formaldehyde molecules where also a softening of J occurs.

In order to illustrate now the consequences of the above findings for macroscopic magnetic quantities such as hysteresis loop and temperature dependence of the coercive field strength, we simulated the magnetization reversal process at finite temperatures using a scheme based on the Monte Carlo (MC) method[36]. To clearly show how the exchange couplings J and the values of MAEs control the magnetization reversal process, the initial coverage of the molecules on the surface in the MC simulations was twice as large as in the DFT calculations, i.e., 12 Fe atoms per unit cell. This corresponds to a coverage density of 3/12 for three closest Fe atoms to the π-conjugated molecules in the unit cell. The calculated hysteresis loops

TABLE II. Calculated MAEs for all systems.

molecule/surface		MAE (meV/atom)		
		[1$\bar{1}$0]	[001]	[110]
clean surface		0.0	2.7	2.3
methyleneborane	(CH$_3$B)	0.0	2.3	3.1
ethene	(C$_2$H$_4$)	0.0	2.1	2.1
methyleneimine	(CH$_3$N)	0.0	1.9	2.4
formaldehyde	(CH$_2$O)	0.0	2.2	3.0

depicted in Fig. 5(a) unambiguously demonstrate a fine tuning of the magnetization reversal process of the surface upon adsorption of the different $\pi-$bonded molecules. The narrowest hysteresis and therefore the smallest coercive field B_c corresponds to the clean surface. On the other hand, this switching field is strongly enlarged upon adsorption of the ethene molecule. It is less affected upon adsorption of methyleneimine and only slightly increased when formaldehyde is employed. Moreover, due to the strong J_1 and J_5 but the very weak J_2 exchange coupling constants for the methyleneborane-surface system, the corresponding switching field closes the gap between the formaldehyde and the methyleneimine cases. We especially stress that for the simulations it is important to take into account all coupling constants individually since an average of the J-values would change the order of the coercive fields. Furthermore, also the temperature dependence [see Fig. 5(b)] of the coercive field strength is always linear and follows the same trend with the strongest J enhancement due to ethene adsorption and the weakest increase in the case of the formaldehyde adsorption. It is very important to emphasize that overall this engineering process of the magnetization hysteresis loop of the molecule-surface systems considered in our study is essentially related to the tuning of the exchange coupling constants J due to the molecule-surface interaction since upon molecular adsorption the calculated MAEs generally decrease with respect to the corresponding clean surface values. To substantiate this observation, note that the largest opening of the magnetisation loop is obtained for ethene with (i) the most significant reduction in MAEs and (ii) a very sizeable increase of the J_1 and J_2 as compared to clean surface reference.

Interestingly, a second source of tuning of the coercive field can be achieved by varying

the concentration of the molecules on the surface as depicted by the inset of Fig. 5(b). In this case N_0 is the total number of Fe atoms per molecule whereas $N_A = 3$ denotes the number of Fe atoms closest to the molecule. In this way the switching field can be fine tuned over a range of 2.2 T. These results unambiguously demonstrate that due to adsorption of organic molecules containing elements with different chemical reactivity, a fine tailoring of the magnetic properties of a ferromagnetic surface can be achieved.
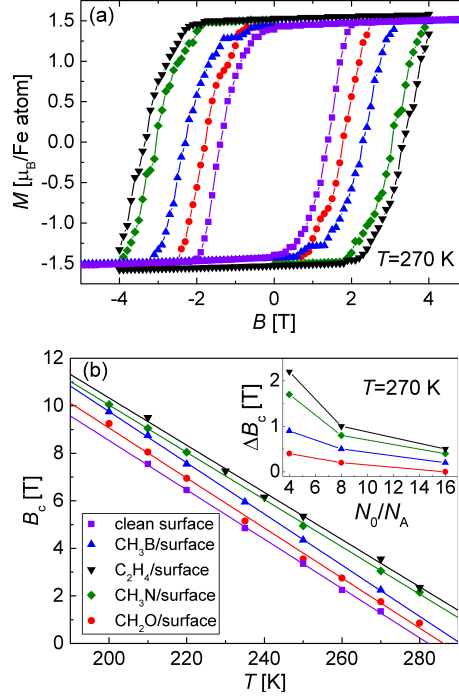

FIG. 5. (a) Calculated hysteresis loops for the chemically functionalized π-conjugated molecules depicted in Fig. 1 when adsorbed on the Fe/W(110) surface and (b) temperature dependence of the coercive field strength for all these systems (Inset: concentration dependence of the difference in coercive field between the respective molecule on the surface and the clean surface). In all cases the clean surface is the softest magnet which can be hardened by adsorption of a chemically functionalized set of organic molecules such that the strongest effect is obtained for ethene.

IV. CONCLUSIONS

To summarize, in this theoretical study we have demonstrated that it is possible to tune the magnetic exchange coupling J of a ferromagnetic surface by tailoring it with a chemically functionalized set of non-magnetic organic molecules containing a single π-bond. Our first-

13

principles study revealed that a hardening or softening of the magnetic exchange coupling between the surface Fe atoms can be achieved depending on the chemical electronegativity of the heteroatom of the functionalized π-bonded molecule. In particular, the strength of the magnetic hardening effect can be specifically tailored by replacing one C atom of the ethene C_2H_4 by B and N ones. Importantly, a magnetic softening of the magnetic exchange coupling can be obtained when using a heteroatom with a large electronegativity such as O. Additionally, this magnetic softening effect can also be reached when a π-bond mediates the coupling between magnetic sites as it is the case for methyleneborane.

Furthermore, the crucial role played by the hybridization between the molecular and surface electronic states (hybridization effect) to tune the magnitude of J was in detail analyzed by comparing the exchange couplings evaluated for the full molecule-surface systems and those calculated from the molecular-induced surface geometry without molecules (geometrical effect).

We also performed Monte Carlo calculations based on a Heisenberg model using exchange coupling constants (J) and magnetocrystaline anisotropy energies (MAE) evaluated from first principles. These simulations demonstrate that the functionalized set of single π-bonded non-magnetic molecules employed in our simulations leads to a selective enhancement of the coercive field strength over a large temperature range. Notably, this tuning process of the magnetization hysteresis upon molecular adsorption is basically due to locally modified exchange coupling constants J induced by the formation of hybrid molecule-surface electronic states.

Overall, our theoretical results clearly demonstrate that the adsorption of organic molecules on a ferromagnetic surface has the potential to engineer the exchange coupling down to the atomic scale and create harder magnetic systems via molecular adsorption. Importantly, our study reveals that carbon atoms mediate a very strong magnetic hardening and this effect can be further enhanced by increasing the spatial extent of the $\pi-$system as already demonstrated in Ref. 20. Furthermore, an additional degree of freedom to enhance or weaken the magnetic exchange interactions of such hybrid organic – magnetic metal interfaces is to couple the spatial extent of the $\pi-$system with an appropriate chemical functionalization as suggested by the present study. To conclude, we expect that the systematic trends identified in our first-principles study are prototypical features for *any* molecule-ferromagnetic surface system and will challenge further research to investigate

14

their consequences for transport properties in spintronic devices.

ACKNOWLEDGMENTS

Appendix A: Heisenberg model

For the molecule-Fe/W(110) systems considered in our study there are in general five different exchange coupling constants for each system (see Fig. 2(e) in the main text). In case of ethene, however, the number of different coupling constants reduces to three since $J_1 = J_2$ and $J_4 = J_5$ due to symmetry. We describe the exchange coupling between the magnetic moments of the Fe atoms by an effective classical Heisenberg Hamiltonian $H = -\sum_{i>j} J_{ij} \, \mathbf{m}_i \, \mathbf{m}_j$ taking into account only the interaction between the nearest neighbor atoms, where $\mathbf{m}_i$ and $\mathbf{m}_j$ stand for the magnetic moments at sites i and j, respectively. The Heisenberg parameters J_{ij} are determined from first-principles by calculating the total energy for a suitable set of particular magnetic configurations for which Fe moments at sites $i = 1, 2, 3$ are flipped. Hence, the total energy difference between the ferromagnetic (FM) and antiferromagnetic (AFM) alignment of surface Fe atoms can be expressed as: $E_{\mathrm{FM}} - E_{\mathrm{AFM}} = -2 \sum_n N_n J_n \mathbf{m}_{i,n} \mathbf{m}_{j,n}$, where $\mathbf{m}_{i,n}$ and $\mathbf{m}_{j,n}$ are the magnetic moments of the coupled Fe atoms at sites i and j and N_n denotes the number of equivalent neighbors of sort n. For example, in Fig. 2(e) of the main text the Fe2 atom has three equivalent couplings J_4 to its unperturbed neighbors ($N_4 = 3$) and one further coupling J_1 to Fe1 ($N_1 = 1$). From this relation a linear system of equations is obtained to determine the different J parameters labeled in Fig. 2(e) of the main text by taking into account a suitable set of antiferromagnetic configurations[37].

15

Appendix B: Monte Carlo simulations

In our Monte Carlo (MC) simulations we used the Heisenberg model containing the exchange interaction between the nearest neighbors (H_{ex}), the uniaxial anisotropy (H_{MAE}) and the Zeeman (H_{Z}) energy terms. The Hamiltonian of the model then reads:

$$
\begin{aligned}
H &= H_{\mathrm{ex}} + H_{\mathrm{MAE}} + H_{\mathrm{Z}} \\
&= -\sum_{i>j} J_{ij}\, \mathbf{S}_i \cdot \mathbf{S}_j - K \sum_i (S_i^x)^2 - \mathbf{B} \sum_i \mathbf{S}_i.
\end{aligned} \tag{B1}
$$

where $\mathbf{S}_i = \mathbf{m}(k_i)/\mu_{\mathrm{B}}$ is the normalized magnetic moment of the i-th Fe atom, μ_{B} is the Bohr magneton, $J_{ij} = J(k_i, k_j)$, and $k_i = 1, 2, 3, 4$ is a site-dependent sort of iron atom Fe1, Fe2, Fe3 and clean surface Fe, respectively (see Fig. 2 of the main text). $\mathbf{B}$ denotes an applied external magnetic field and K represents the magnetocrystaline anisotropy parameter. Values for K, $J(1,2) = J_1, J(1,3) = J_2, J(1,4) = J_3, J(2,4) = J_4$ and $J(3,4) = J_5$ are specified in the main text. For the case of a clean monolayer Fe/W(110) it is assumed that $k_i = 4$ for any i-th lattice site. For simplicity, we assumed that the different sorts of molecules are all distributed regularly over the surface.

The MC simulations were performed by using a two-dimensional regular lattice (see Fig. 2 of the main text) with periodic boundary conditions. Depending on the coverage density of the molecules the lattice extent is slightly adapted to fit the periodic boundary conditions. The average size of the simulated domain is about 90×90 spins. In order to enhance the efficiency of the MC simulations during the magnetization reversal process, we employed a combined sampling algorithm[36]. The combined sampling consists of a set of different trial steps in each MC step. In our simulations we used a combined sampling with three uniform trial steps and one small trial step, for details see Ref. 36. For the simulation of the annealing and the magnetization reversal process we utilized 10^4 MC steps for the system relaxation and 10^5 steps for the statistical sampling at each temperature or applied field step. The magnetization curves and the temperature dependence of the coercive field are obtained by averaging over ∼100 independent runs.

The presence of different types of defects which represent nucleation centers can substantially reduce the switching field. Thereby, in practice the coercive field might be lower than that predicted by the MC simulations, but the basic trends will remain unaffected. A detailed discussion of these issues require more complex and accurate theoretical models

16

and is beyond the scope of this work. In conclusion, the aim of the MC calculations was to present a qualitative description of the magnetization properties of several chemically functionalized $\pi-$bonded molecules adsorbed on the ferromagnetic Fe/W(110) surface.

Appendix C: Structural Data

TABLE III. Distances (in Å) for the different systems investigated in this study. Note that the clean surface Fe-Fe distance is 2.75Å. cs stands for 'clean surface' and h for 'hetero'.

molecule/surface		Fe1-Fe2	Fe1-Fe3	Fe1-cs	Fe2-cs	Fe3-cs	C-Fe1	C-Fe3	h-Fe1	h-Fe2	h-Fe3
methyleneborane	(CH_3B)	2.86	2.88	2.71	2.75	2.69	2.12	2.21	2.13	1.98	2.14
ethene	(C_2H_4)	2.61	2.61	2.91	2.77	2.77	2.11	2.25	2.11	2.25	3.10
methyleneimine	(CH_3N)	2.71	2.65	2.85	2.78	2.77	2.11	2.19	2.05	2.01	3.00
formaldehyde	(CH_2O)	2.75	2.65	2.85	2.79	2.77	2.10	2.15	2.03	2.05	2.99

* r.friedrich@fz-juelich.de

† n.atodiresei@fz-juelich.de

[1] I. Žutić, J. Fabian, and S. D. Sarma, Rev. Mod. Phys. **76**, 323 (2004).

[2] L. Bogani and W. Wernsdorfer, Nat. Mater. **7**, 179 (2008).

[3] V. A. Dediu, L. E. Hueso, I. Bergenti, and C. Taliani, Nat. Mater. **8**, 707 (2009).

[4] N. Atodiresei, and K. V. Raman, MRS BULLETIN **39**, 596 (2014).

[5] V. Dediu, M. Murgia, F. C. Matacotta, C. Taliani, and S. Barbanera, Solid State Commun. **122**, 181 (2002).

[6] Z. H. Xiong, D. Wu, Z. Valy Vardeny, and J. Shi, Nature **427**, 821 (2004).

[7] K. V. Raman, A. M. Kamerbeek, A. Mukherjee, N. Atodiresei, T. K. Sen, P. Lazić, V. Caciuc, R. Michel, D. Stalke, S. K. Mandal, S. Blügel, M. Münzenberg, and J. S. Moodera, Nature **493**, 509 (2013).

[8] X. Sun, M. Gobbi, A. Bedoya-Pinto, O. Txoperena, F. Golmar, R. Llopis, A. Chuvilin, F. Casanova, and L. E. Hueso, Nat. Commun. **4**, 2794 (2013).

17

[9] M. Urdampilleta, S. Klyatskaya, J.-P. Cleuziou, M. Ruben, and W. Wernsdorfer, Nat. Mater. **10**, 502 (2011).

[10] R. Vincent, S. Klyatskaya, M. Ruben, W. Wernsdorfer, and F. Balestro, Nature **488**, 357 (2012).

[11] S. Sanvito, Chem. Soc. Rev. **40**, 3336 (2011).

[12] D. Sun, E. Ehrenfreund, and Z. V. Vardeny, Chem. Commun. **50**, 1781 (2014).

[13] M. Cinchetti, K. Heimer, J.-P. Wüstenberg, O. Andreyev, M. Bauer, S. Lach, C. Ziegler, Y. Gao, and M. Aeschlimann, Nat. Mater. **8**, 115 (2009).

[14] C. Barraud, P. Seneor, R. Mattana, S. Fusil, K. Bouzehouane, C. Deranlot, P. Graziosi, L. Hueso, I. Bergenti, V. Dediu, F. Petroff, and A. Fert, Nat. Phys. **6**, 615 (2010).

[15] N. Atodiresei, J. Brede, P. Lazić, V. Caciuc, G. Hoffmann, R. Wiesendanger, and S. Blügel, Phys. Rev. Lett. **105**, 066601 (2010).

[16] J. Brede, N. Atodiresei, S. Kuck, P. Lazić, V. Caciuc, Y. Morikawa, G. Hoffmann, S. Blügel, and R. Wiesendanger, Phys. Rev. Lett. **105**, 047204 (2010).

[17] N. M. Caffrey, P. Ferriani, S. Marocchi, and S. Heinze, Phys. Rev. B **88**, 155403 (2013).

[18] N. Atodiresei, V. Caciuc, P. Lazić, and S. Blügel, Phys. Rev. B **84**, 172402 (2011).

[19] M. Callsen, V. Caciuc, N. Kiselev, N. Atodiresei, and S. Blügel, Phys. Rev. Lett. **111**, 106805 (2013).

[20] J. Brede, N. Atodiresei, V. Caciuc, M. Bazarnik, A. Al-Zubi, S. Blügel, and R. Wiesendanger, Nat. Nanotech. **9**, 1018 (2014).

[21] J. E. Bickel, F. Meier, J. Brede, A. Kubetzka, K. von Bergmann, and R. Wiesendanger, Phys. Rev. B **84**, 054454 (2011).

[22] R. Decker, J. Brede, N. Atodiresei, V. Caciuc, S. Blügel, and R. Wiesendanger, Phys. Rev. B **87**, 041403(R) (2013).

[23] R. Decker, M. Bazarnik, N. Atodiresei, V. Caciuc, S. Blügel, and R. Wiesendanger, J. Phys.: Condens. Matter **26**, 394004 (2014).

[24] T. Andersen and W. Hübner, Phys. Rev. B **74**, 184415 (2006).

[25] N. Atodiresei, V. Caciuc, P. Lazić, and S. Blügel, Phys. Rev. Lett. **102**, 136809 (2009).

[26] P. Hohenberg and W. Kohn, Phys. Rev. **136**, B864 (1964).

[27] W. Kohn and L. J. Sham, Phys. Rev. **140**, A1133 (1965).

[28] G. Kresse and J. Hafner, Phys. Rev. B **49**, 14251 (1994).

[29] G. Kresse and J. Furthmüller, Phys. Rev. B **54**, 11169 (1996).

[30] P. E. Blöchl, Phys. Rev. B **50**, 17953 (1994).

[31] J. P. Perdew, K. Burke, and M. Ernzerhof, Phys. Rev. Lett. **77**, 3865 (1996).

[32] Y. Mokrousov, N. Atodiresei, G. Bihlmayer, and S. Blügel, Int. J. Quant. Chem. **106**, 3208 (2006).

[33] A. L. Allred and E. G. Rochow, Journal of Inorganic and Nuclear Chemistry **5**, 264 (1958).

[34] K. Momma and F. Izumi, J. Appl. Cryst. **44**, 1272 (2011).

[35] We note that the enhanced coupling constants are partially due to the reduced magnetic moments for the hybrid molecule-surface systems. However the inclusion of the size of the magnetic moments into the coupling constant which would then be expressed as an energy does not change the conclusions of our study.

[36] D. Hinzke and U. Nowak, Comput. Phys. Commun. Proceedings of the Europhysics Conference on Computational Physics CCP 1998, **121**–**122**, 334 (1999).

[37] It should however be mentioned that due to the redundancy within our model we are able to estimate the errorbar for the calculated J values to about 3 meV/μ_B^2.